ELSEVIER

Sensors and Actuators B 72 (2001) 35–40

SENSORS AND ACTUATORS B CHEMICAL

www.elsevier.nl/locate/sensorb

A new type of amperometric oxygen sensor based on a mixed-conducting composite membrane

Zuoyan Peng[a], Meilin Liu[a,*], Ed. Balko[b]

[a]*School of Materials Science and Engineering, Georgia Institute of Technology, Atlanta, GA 30332-0245, USA*
[b]*Engelhard Corporation, 101 Wood Avenue, Iselin, NJ 08830-0770, USA*

Received 5 March 2000; received in revised form 24 July 2000; accepted 25 July 2000

Abstract

A new type of amperometric oxygen sensor has been developed in which a dense Pt-YSZ composite layer, a mixed ionic–electronic conductor (MIEC) membrane, is used as the diffusion barrier. Accelerated materials stability tests in the exhaust of a gas-fired engine indicate that yttria-stabilized zirconia (YSZ) with fluorite structure has excellent stability while the stability of $La_{0.9}Sr_{0.1}Ga_{0.2}Mg_{0.8}O_3$ (LSGM) is questionable. A dense Pt-YSZ composite layer has been prepared on a YSZ electrolyte using nanoparticles of platinum, derived from a sol–gel process. The fabricated sensors based on a bi-layer structure, Pt-YSZ/YSZ, exhibit well-defined diffusion-limited currents for oxygen concentrations up to 6% and the current responses depend linearly on oxygen concentration. The developed sensor is anticipated to have excellent chemical, microstructural, and thermal stability because of the remarkable stability of a dense composite layer consisting of YSZ and Pt.

Keywords: Amperometric oxygen sensor; Pt-YSZ composite layer; Sol–gel process

1. Introduction

With continuous improvements and stringency in environmental regulations and advances in emission control technology, there is an intense demand for low-cost, high-sensitivity gas sensors for better control of combustion in order to minimize pollutant emission while improving energy efficiency. One of the most important gas sensors is the solid-state oxygen sensor for control of air-to-fuel ratio in automobiles, furnaces and other combustion processes [1–5]. While potentiometric oxygen sensors have been widely used for control of stoichiometric combustion, they do not have adequate sensitivity to changes in oxygen concentration, when the partial pressure of oxygen in sample gas is too close to that of reference gas (typically air) because of the logarithmic response. On the other hand, an amperometric (or a limiting current-type) oxygen sensor exhibits a linear dependence on oxygen concentration in the sample gas. Amperometric sensors are, therefore, more suitable for control of lean-burn combustion.

For a traditional amperometric oxygen sensor, a porous ceramic layer (or a cap with a laser-drilled hole) is used as diffusion barrier to control the inflow of oxygen [6–8]. The characteristics of such a sensor depend critically on the microstructure of the diffusion barrier (or the size of the hole). The disadvantages associated with this design are that, the pore or hole dimension is difficult to control and the pores or hole can be readily blocked by particulate in the sample gas to be monitored. To overcome these difficulties, mixed-conducting ceramic membranes have been used as the diffusion barrier for amperometric sensors [9–11]. To date, however, the mixed conductors were selected from the group consisting of lanthanum strontinum manganese oxide (LSM), lanthanum strontium cobalt oxide (LSC), and terbia-yttria stabilized zirconia (Tb-YSZ). The stability of these mixed conductors is questionable and the reliability of a solid-state gas sensor depends mainly on the stability of the sensing components, particularly the one in contact with exhaust. For example, the stability and reliability of a sensor based on a mixed-conducting membrane depends critically on the stability of the dense mixed conducting membrane exposed to exhaust containing various pollutants at temperatures up to 1100°C. While Tb-YSZ was reported to be stable in a sulfur-containing atmosphere [12], LSM and LSC are not very stable in gases containing unburned hydrocarbons and sulfur-containing compounds at high temperatures [11]. Accordingly, the performance of a sensor based on these mixed conductors may change during the course of operation, leading to drift in sensor output (or lack of

* Corresponding author. Tel.: +1-404-894-6114; fax: +1-404-894-9140.
E-mail address: meilin.liu@mse.gatech.edu (M. Liu).

0925-4005/01/$ – see front matter
PII: S0925-4005(00)00629-8

stability) and even to sensor failure. In addition to the chemical stability, the transport properties of the mixed conductors used as diffusion barrier must not change significantly over the oxygen partial pressure range of interest, in order to achieve a wide–range oxygen detection. Therefore, the mixed conductors used as diffusion barrier must have excellent stability under operating conditions to achieve stability, reliability and reproducibility.

Recently, a dense composite membrane consisting of platinum and YSZ was used as the diffusion barrier for amperometric oxygen sensors because of its high chemical and microstructural stability [13]. The mechanism of mixed ionic–electronic conduction in a metal-ceramic composite such as Pt-YSZ is discussed in detail elsewhere [14]. In this paper, the stability and performance characteristics of amperometric oxygen sensors based on a Pt-YSZ composite membrane are discussed.

2. Experimental

2.1. Preparation of electrolyte pellets

$La_{0.9}Sr_{0.1}Ga_{0.2}Mg_{0.8}O_3$ (LSGM) and yttria-stabilized zirconia (YSZ) were studied as electrolyte for the amperometric sensors. LSGM samples were prepared as described elsewhere [15]. Stoichiometric amounts of $La_2(CO_3)_3{\cdot}xH_2O$, Ga_2O_3, $SrCO_3$ and MgO were ball-milled in ethanol for 24 h and calcined at 1300°C in air for 5 h. X-ray powder diffraction (Philips, PW1800) was used to examine the phase composition of the calcined product. In case of incomplete calcination, ball-milling and calcination were repeated until pure perovskite phase was obtained. Powders with perovskite phase were crushed using agate mortar and pestle and then ball-milled in ethanol for another 24 h. The resulting fine powder was pressed into pellets (diameter 20 mm and thickness 2–3 mm) and sintered at 1450°C for 10 h to get dense LSGM pellets. Similarly, powder of yttria-stabilized zirconia (TZ-8 from Tosoh) was pressed to pellets using the same die and sintered at 1350°C for 5 h. The microstructures of prepared pellets were characterized using a scanning electron microscope (SEM, Hitachi S-800). To measure the electrical properties, both surfaces of each sintered LSGM and YSZ pellets were grounded and ultrasonically cleaned before a paste of Pt electrode was screen-printed on them. Pellets with printed Pt electrodes were then fired at 920°C for 10 min to form porous Pt electrodes.

2.2. Preparation of fine platinum powders and Pt-YSZ mixed powder

In a typical experiment, 20 g Pt powder (Engelhard) was dissolved into 120 ml HCl/HNO_3 (volume ratio is 3:1) to obtain a clear $PtCl_4$ solution with dark orange color, which was then kept at 80–90°C, until its volume was reduced to about 80 ml. To this solution, 30 g polyethylene glycol (PEG, F. W. 20,000, Alfa) was added under stirring at 80–90°C, until a viscous gel was formed, which was then dried using an IR lamp. The dried gel was grounded into powder and fired at 500°C for 2 h to obtain sub-micron particles of platinum. Alternatively, the prepared $PtCl_4$ solution, yttrium nitrate ($Y(NO_3)_3{\cdot}6H_2O$, Johnson Matthey) and zirconium dichloride oxide ($ZrOCl_2.8H_2O$, Alfa) were used as precursors to prepare fine Pt-YSZ composite powders using a sol–gel process. Calculated amount of precursors were dissolved into water and appropriate amount of citric acid (the molar ratio of citric acid to metal ions was 2:1) and PEG (about 50% of the weight of metal and metal oxide) were added into this solution, which was stirred until it became clear. The solution was then heated up to 80°C to evaporate solvent and to obtain a gel, which was further dried using an infrared heating bulb. The dried gel was crushed into powders using agate mortar and pestle and followed by calcination at 650°C for 2 h to obtain Pt-YSZ composite powders.

The volume fraction of each phase in the Pt-YSZ composite must be appropriate, in order for the layer to function as a mixed-conducting membrane. For a three-dimentional, two-phase composite MIEC (like Pt-YSZ), the percolation threshold is found at 1/3 volume fraction of the more conductive phase (Pt) [14]. The ambipolar conductivity is relatively high when the volume fraction of each phase is in the range of 1/3–2/3, so that both phases are continuous. Accordingly, the volume fraction of Pt in the composite was selected to be 40%. Since the density of platinum is 21.45 g/cm^3 and that of YSZ is 5.89 g/cm^3, the weight ratio of Pt to YSZ was kept at 2.43.

2.3. Preparation of YSZ/Pt-YSZ two-layer structures using uniaxial pressing

In a typical preparation, 5.0 g YSZ (TZ-8Y, TOSOH) powder was mixed with 1 g PVA solution (5 wt.% in water) and grounded until the binder was dispersed uniformly. In another mortar, 1.0 g Pt (sol–gel powder) was mixed with 0.412 g YSZ and grounded in ethanol for 60 min to ensure uniform mixing, followed by the addition of 0.245 g PVA solution (5 wt.% in water) and grounded for another 10 min. Initially, YSZ-8 (0.200 g) was put in die and then the piston was turned back and forth for 3–4 times, followed by repress at 0.4 t for 3 s. Then, Pt-YSZ (0.100 g) was spread on the top of the repressed YSZ in die, the piston was turned back and forth for several times to make sure the Pt-YSZ powder is uniform and covers the surface of repressed YSZ completely. Finally, the powder was pressed at 3 t holding for 20 s to obtain a pressed two-layer pellet, which was then buried in YSZ powder and sintered at 1630°C for 5 h.

2.4. Electrical characterization

A computerized impedance analysis system, consisting of a Frequency Response Analyzer (Solartron 1255) and an

Electrochemical Interface (Solarton 1286), was used to measure the impedance of the cells in air at temperatures varying from 600 to 800°C in the frequency range from 65,000 to 0.1 Hz. The sensors were tested in a tube furnace and the composition of sample gases was analyzed using an on-line gas chromatograph (GC, varian 3800).

3. Results and discussion

3.1. Microstructure of powder and pellet electrolytes

Shown in Fig. 1(A) is an SEM view of the prepared LSGM powder (calcined at 1300°C in air for 5 h), indicating that the average particle size is about 1.4 μm. The surface view of an LSGM pellet sintered at 1450°C for 10 h, as shown in Fig. 1(B), indicates that the sintered density is greater than 97% of the theoretical value and the average grain size is about 6 μm. Fig. 2(A) shows a SEM view of the YSZ powder as received from Tosoh with particle sizes of about 100 nm. The surface view of a dense YSZ pellet, pressed using the Tosoh powder and sintered at 1350°C for 4 h, as shown in Fig. 2(B), indicates that the average grain size is about 1.5 μm with sintered density close to 100%.

3.2. Stability of the electrolytes

To study the stability of the electrolyte materials for the sensor applications, LSGM and YSZ samples were immersed in the exhaust of a gas-fired engine operated at

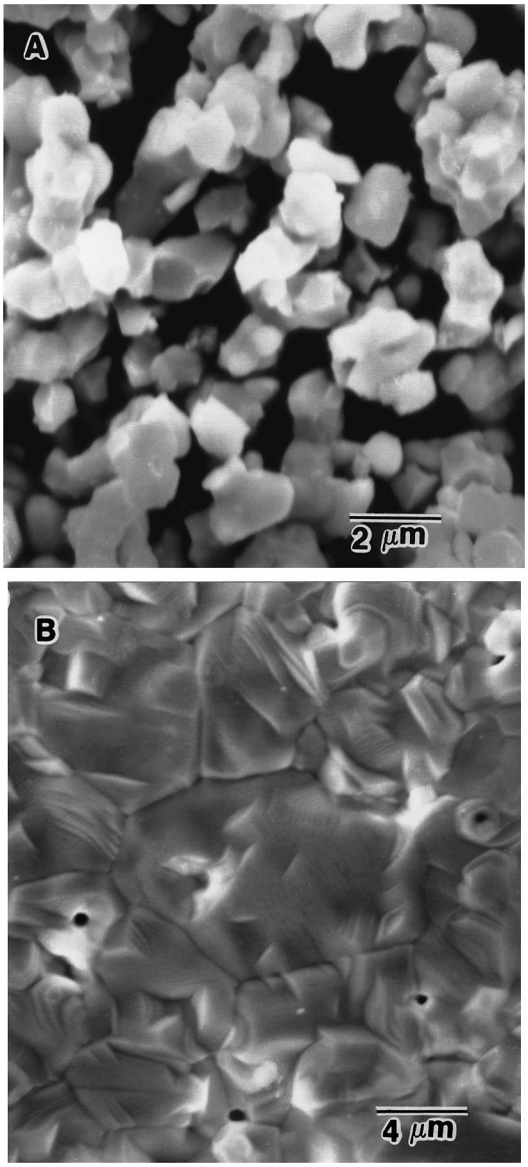

Fig. 1. SEM micrographs of LSGM samples: (A) powder calcined at 1300°C in air for 5 h and (B) surface view of a pellet sintered at 1450°C for 10 h.

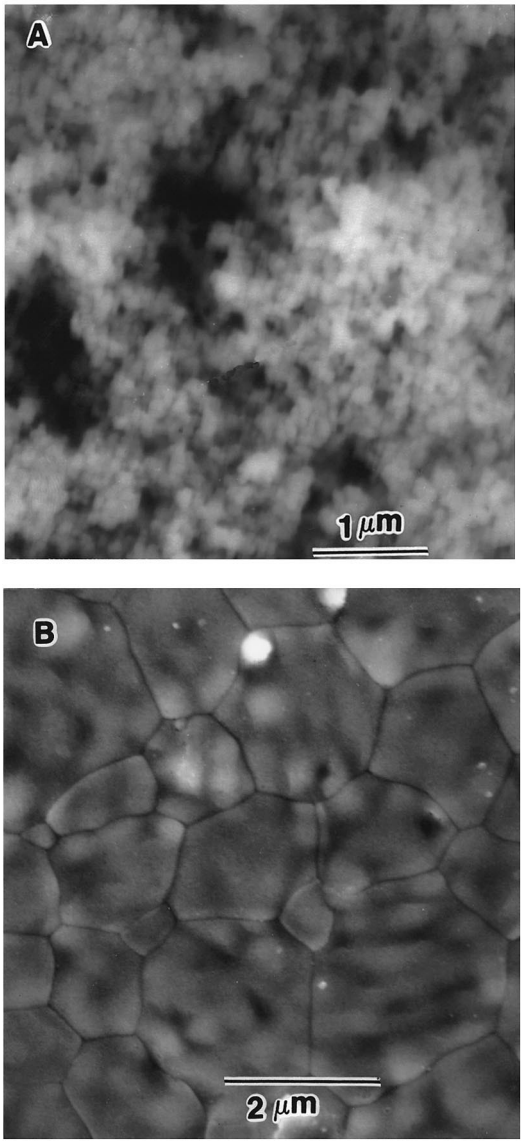

Fig. 2. SEM micrographs of YSZ-8 samples: (A) powder as received from Tosoh and (B) surface views of a pellet sintered at 1350°C for 4 h.

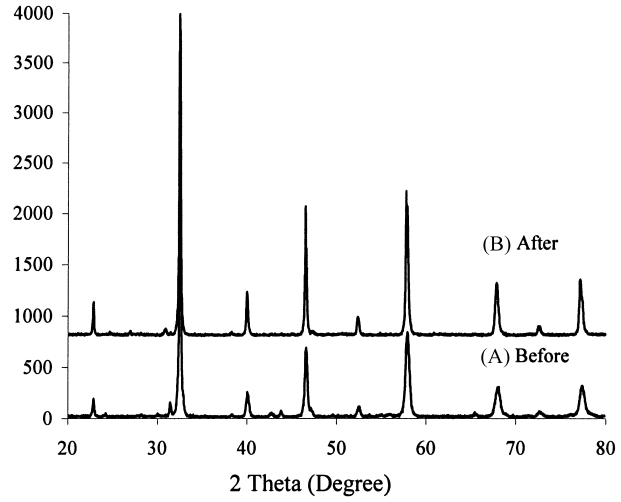

Fig. 3. XRD patterns of an LSGM sample before (A) and after (B) exposed to the exhaust of a gas-fired engine with a thermal history of 50 h at 820°C, 90 h at 840°C and 10 h at 850°C.

stoichiometric combustion with a thermal history of 50 h at 820°C, 90 h at 840°C, and 10 h at 850°C. The XRD patterns of LSGM and YSZ pellets before and after the aging test are shown in Figs. 3 and 4, respectively; it appears that there are no observable phase changes for both LSGM and YSZ samples. The impedance spectra of LSGM samples *before* and *after* the aging test were measured at different temperatures in air and the conductivities of LSGM and YSZ, calculated from the impedance data are summarized in Fig. 5. Clearly, the conductivities of YSZ are within experimental error while the conductivities of LSGM, indeed, degraded considerably during the aging test, implying that the stability of LSGM for the sensor applications may be questionable.

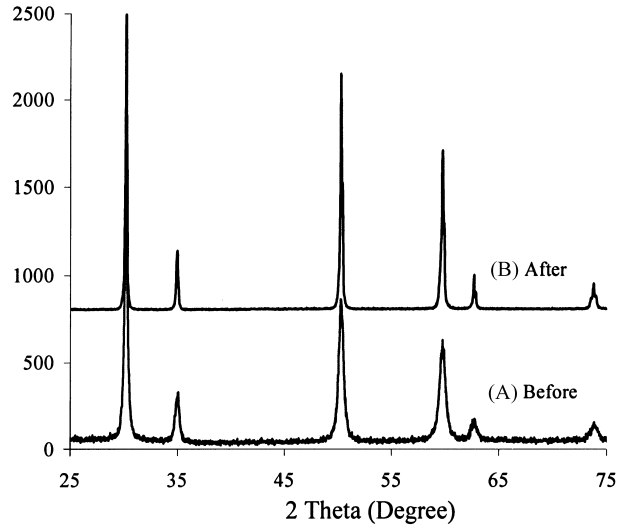

Fig. 4. XRD patterns of YSZ-8 before (A) and after (B) exposed to the exhaust of a gas-fired engine with a thermal history of 50 h at 820°C, 90 h at 840°C and 10 h at 850°C.

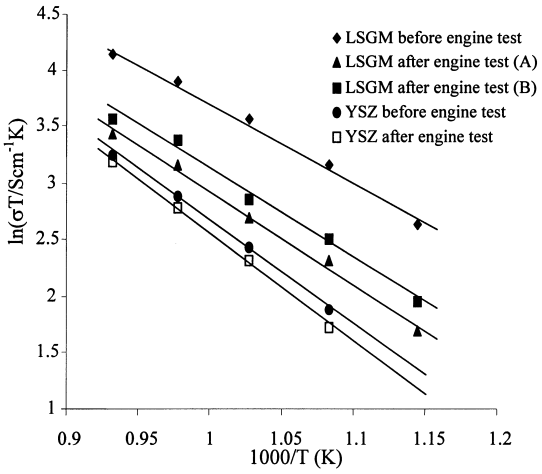

Fig. 5. Conductivities of YSZ-8 and LSGM samples before and after the engine aging test as calculated from the impedance spectra measured at different temperatures.

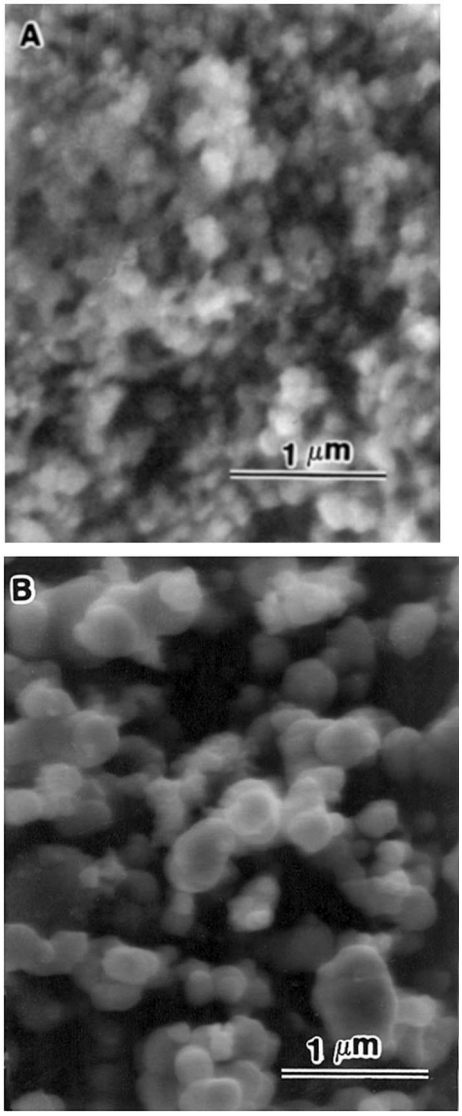

Fig. 6. Morphologies of platinum powders: (A) derived from a sol–gel process and (B) as received from Engelhard.

3.3. Microstructure of the composite layer

Fig. 6 shows the morphologies of the sol–gel derived Pt powder (A) and the Pt powder as received from Engelhard (B). It can be seen that the sol–gel derived Pt powder is very uniform and the average particle size is about 0.1 μm. The particle size of the Pt powder from Engelhard varies from 0.1 to 0.6 μm. The platinum powders were mixed with Tosoh YSZ powders to form YSZ/Pt-YSZ bi-layer structures. The cross-sectional views of the two samples shown in Fig. 7 indicate that the Pt-YSZ composite layer using sol–gel derived platinum powder (Fig. 6A) is reasonably dense (Fig. 7A), whereas that using coarse platinum powder (Fig. 6B) is porous (Fig. 7B).

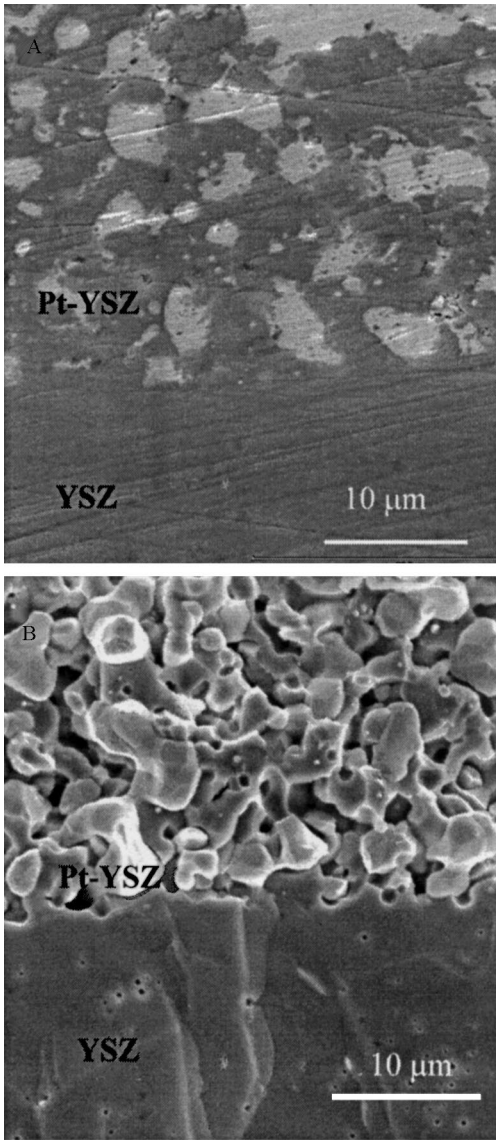

Fig. 7. Cross-sectional views of Pt-YSZ composite layers prepared using (A) the fine platinum powder derived from a sol–gel process and (B) the coarse platinum powder as received from Engelhard.

In addition, Pt-YSZ composite powders prepared using a sol–gel method were used to press the bi-layer pellets and then sintered in air for 4 h at 1400, 1500 and 1600°C, respectively. While the surface of each composite layer appears to be dense, the cross-sectional views clearly indicate that they are porous, even for the sample sintered at 1600°C for 4 h. In order to reduce the sintering temperature and increase the sintered density, some other oxides with low melt-point such as SnO_2 and Bi_2O_3 were used as additives. The results indicate that the addition of Bi_2O_3 does not improve the density and the addition of SnO_2 has detrimental effect on the electric properties, although it indeed improved the sintered density.

3.4. Sensor performance

Shown in Fig. 8(A) are some typical current-voltage (*I–V*) curves of a sensor with a configuration of Pt/YSZ/Pt-YSZ, as measured in different oxygen concentrations. The Pt-YSZ composite layer was prepared using Pt fine powder and YSZ. It can be seen that the diffusion-limited currents are flat for oxygen concentrations up to 6%. The diffusion-limited current (measured at 1 Volt) depend linearly on the oxygen concentrations as shown in Fig. 8(B). However, it is not as

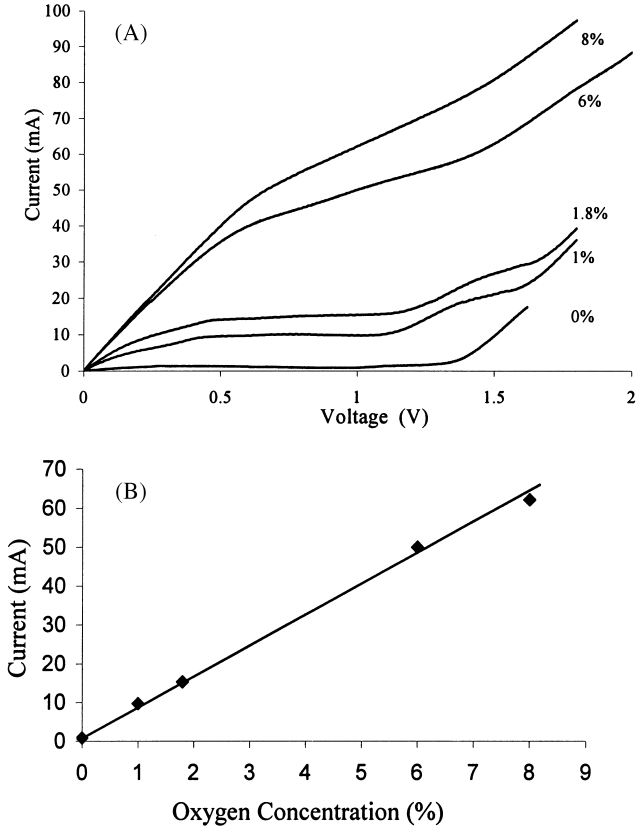

Fig. 8. (A) *I–V* curves of a sensor with configuration of Pt/YSZ/Pt-YSZ as measured in different oxygen concentrations and (B) calibration curve for the sensor, i.e. the diffusion-limited currents (measured at 1 Volt) versus the oxygen concentrations.

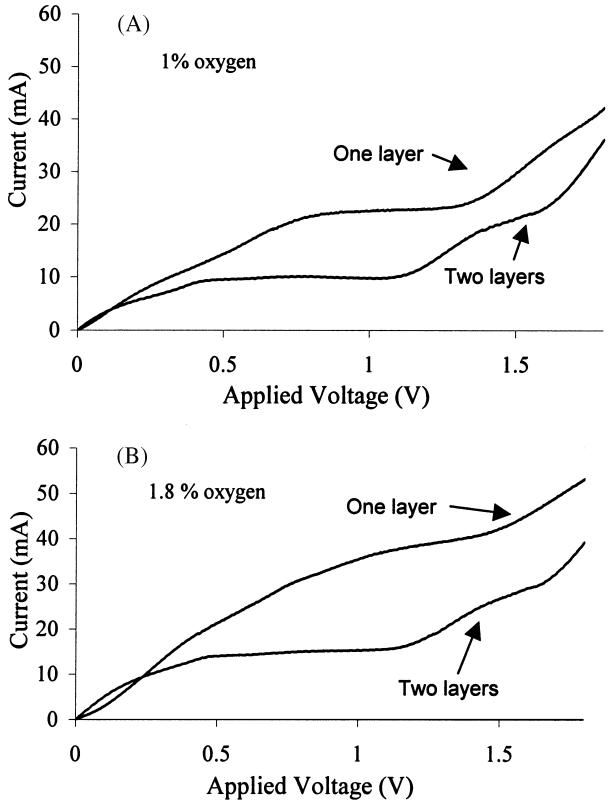

Fig. 9. *I–V* curves of a sensor (Pt/YSZ/Pt-YSZ) with counter electrodes of different thicknesses prepared by brush painting as measured in (A) 0.5% and (B) 1% O_2.

good as expected for high concentrations of oxygen. Possible causes include: (a) the density of the top Pt-YSZ layer was inadequate, (b) the sheet resistance of the counter electrode was too large and (c) the thickness ratio of the YSZ electrolyte to the Pt-YSZ layer was inappropriate. In order to determine the influence of counter electrode on sensor performance, the *I–V* curves of a sample with one layer of counter electrode was measured at 800°C. Then, a second layer of Pt was applied to increase the thickness of the counter electrode and the *I–V* curves were measured under the same conditions. The results are shown in Fig. 9, indicating that the thickness of the counter electrode has some influence on sensor performance. The electrode should be sufficiently thick so that the sheet resistance of the electrode is sufficiently small.

Also, the thickness ratio of the YSZ to Pt-YSZ was changed from 12:1 to 2:1 and the results show that the thickness ratio of the YSZ electrolyte to Pt-YSZ layer did not have significant effect on sensor performance in the range of thickness ratio studied under the test conditions.

4. Conclusions

A new limiting-current type oxygen sensor has been developed using a dense composite layer of Pt and YSZ as the diffusion barrier. While the stability of YSZ with fluorite structure is excellent, the stability of LSGM may be questionable for the sensor application in the exhaust of a gas-fired engine. A sol–gel process has been developed for the preparation of uniform sub-micron particles of platinum, which are important in the formation of a functional bi-layer structure, consisting of a layer of YSZ and a layer of Pt-YSZ composite. It is found that the fabricated sensors based on a Pt/YSZ/Pt-YSZ structure exhibit well-defined diffusion-limited currents for oxygen concentrations up to 6% and the dependence of the current responses on oxygen concentration is approximately linear. The thickness ratio of YSZ to Pt-YSZ does not have significant effect on sensor performance in the range of thickness ratio studied, implying that the currents are indeed controlled by the Pt-YSZ composite layer for the samples studied.

Acknowledgements

The financial support of this research by Engelhard Corporation is gratefully acknowledged.

References

[1] H. Dietz, Gas-diffusion-controlled solid-electrolyte oxygen sensors, Solid State Ionics 6 (1982) 175–183.
[2] T. Takeuchi, Oxygen sensors, Sensors and Actuators 14 (1988) 109–124.
[3] S. Matsurra, New Developments and application of gas sensors in Japan, Sensors and Actuators B 13-14 (1993) 7–11.
[4] K. Ishibashi, T. Kashima, A. Asada, Planar type of limiting current oxygen sensor, Sensors and Actuators B 13-14 (1993) 41–44.
[5] A.Q. Pham, R.S. Glass, Characteristics of the amperometric oxygen sensor, J. Elentrochem. Soc. 144 (11) (1997) 3929–3934.
[6] T. Takeuchi, I. Igarashi, Limiting current type oxygen sensor, Chem. Sensor Technol. 1 (1988) 79–95.
[7] T. Usui, K. Nuri, M. Nakazawa, H. Osanai, Output characteristics of a gas-polarographic oxygen sensor using a zirconia electrolyte in the knudsen diffusion region, Jpn. J. Appl. Phys. 26 (1987) L2061–L2064.
[8] K. Saji, H. Kondo, H. Takahashi, T. Takeuchi, I. Igarashi, Influence of H_2O, CO_2 and various combustible gases on the characteristics of a limiting current-type sensor, J. Appl. Electrochem. 18 (1988) 757–762.
[9] F.H. Garzon, B. Chung, I.D. Raistrick, E.L. Brosha, Solid State Oxygen Sensor, U.S. Patent No. 5,543,025, (1996).
[10] F. Garzon, I. Raistrick, E. Brosha, R. Houlton, B.W. Chung, Dense diffusion barrier limiting current oxygen sensors, Sensors and Actuators B 50 (1998) 125–130.
[11] M. Liu, I. Bae, A. Joshi, Amperometric sensors based on ceramic membranes, in: M. Butler, T. Rico (Eds.), Proceedings of The Electrochemical Society Symposium on Chemical Sensors II, Pennington, NJ., Vol. 7, 1993, pp. 421–427.
[12] E.L. Brosha et al., Sulfur resistant oxygen sensors for industrial boiler control, in: Proceedings of the Symposium on Solid State Ionic Devices, Vol. 13, 1999, pp. 37–38.
[13] M. Liu, Oxygen sensor and emission control system, U.S. patent application, serial no. 09/453, 283, 12/2/99.
[14] Z. Wu, M. Liu, Modeling of Ambipolar Transport Properties of Composite Mixed Conductors, Solid State Ionics 93 (1997) 65–84.
[15] F. Chen, M. Liu, Transition metal oxides doped LSGM as electrodes for LSGM electrolytes, J. Solid State Electrochem. 3 (1998) 7–14.